1965ApJ...141.1019B

STUDIES IN STELLAR EVOLUTION. I. THE INFLUENCE OF INITIAL CNO ABUNDANCES IN A STAR OF MASS 2.3

PETER BODENHEIMER, J. E. FORBES, NANCY L. GOULD, AND L. G. HENYEY
Berkeley Astronomical Department, University of California

Received October 26, 1964

ABSTRACT

A series of evolutionary sequences have been calculated for a configuration of mass 2 3 $M_\odot$. They cover late pre-main-sequence and main-sequence evolution and differ in their initial chemical compositions. Sequence I begins with concentrations of C, N, and O similar to observed atmospheric values published for stars predominantly of Population I. The C/N and O/N ratios are considerably in excess of their equilibrium values, and there is found to be a pre-main-sequence adjustment period of carbon burning causing an additional pre-main-sequence dip in luminosity on the Hertzsprung-Russell diagram. Sequence IV shows that the dip becomes less marked if the total heavy-element concentration is reduced. Sequence II begins with nearly equilibrium abundances of C^{12} and N^{14} and the carbon dip is not seen. Sequence III illustrates the effect of increasing the O/N ratio and confirms that O^{16} is only very gradually converted to CN isotopes.

In a series of appendices we describe the physical approaches and approximations used in these calculations. They are intended to supplement the basic discussion of the numerical technique. They treat the equation of state, opacity, chemical composition changes due to hydrogen burning, chemical homogenization of convective regions, and the obtaining of a starting configuration for an evolutionary sequence.

I. PRELIMINARY REMARKS

In a recent report Henyey, Forbes, and Gould (1964; hereinafter called "HFG")[1] described a numerical technique for the automatic calculation of stellar evolution. The research program which has been organized to exploit this technique includes an evolutionary sequence for a configuration of mass 2.3 times the mass of the Sun. Such a sequence provides some calibration of and check on the parameters involved through a comparison with the observed characteristics of Sirius. The results for one such sequence suggested certain additional parallel sequences for the same mass but for differing compositions. Collectively the various conclusions and results of these computations form the subject of this report. It is the first of a series, based on the above-mentioned method, which will appear periodically in the literature.

In HFG it was emphasized that the discussion there was confined to the logical approach to the problem of evolutionary calculations and any discussion of physical details was therefore deliberately avoided as irrelevant to the technique being described. In the present investigation it is of course essential to discuss the physical laws on which the calculation is based. Since these form the basis of future investigations as well as of the study of mass 2.3 $M_\odot$ presented here, we discuss the details in appendices which are logically independent of the main text.

II. INTRODUCTION

The conditions specified at the beginning of an evolutionary sequence of models must include a complete list of concentrations of those species whose abundances influence any of the physical parameters required in the calculation. With reference to the nuclear reactions prevailing at or near main-sequence phases the relevant species are H^1, He^3, He^4, C^{12}, C^{13}, N^{14}, and O^{16}. All of these are involved in hydrogen burning, directly or indirectly, the CNO isotopes being relatively more significant for masses larger than

---

[1] In that paper, p. 310, 16th line after equation (27), the following typographical error should be corrected: *for* $S_c^{(2)}$ and $S_c^{(2)}$ *read* $S_c^{(2)}$ and $S_e^{(2)}$.

that of the Sun and also for post-main-sequence phases of evolution. During the fully developed operation of the CNO bi-cycle the various nuclear species are very nearly in statistical equilibrium. In strict equilibrium the concentrations bear ratios to each other which are functions only of the temperature. Such a regime is achieved only after any initial readjustment required to convert initially existing (or, computationally, initially specified) concentrations to their equilibrium values.

A natural choice for the initially specified concentrations is one based on published values determined principally from the analyses of stellar spectra (Population I). The relative abundances of the CNO isotopes so determined are definitely very different from what may be expected in an equilibrium regime. Specifically, the C/N and the O/N ratios are considerably in excess of their equilibrium values. In a computation based on such values there will be a period of readjustment prior to the fully developed operation of the CNO bi-cycle.

TABLE 1

INITIAL CHEMICAL COMPOSITION

SPECIES	CONCENTRATION IN GRAMS PER GRAM OF MIXTURE			
	Sequence I	Sequence II	Sequence III	Sequence IV
H	0 68	0 68	0 68	0 69
He^4	0 29	0 29	0 29	0 29
C^{12}	4 2 $\times 10^{-3}$	1 6 $\times 10^{-4}$	1 6 $\times 10^{-4}$	2 8 $\times 10^{-3}$
C^{13}	5 4 $\times 10^{-5}$	5 4 $\times 10^{-5}$	5 4 $\times 10^{-5}$	3 6 $\times 10^{-5}$
N	1 45 $\times 10^{-3}$	5 49 $\times 10^{-3}$	1 359$\times 10^{-2}$	9 67$\times 10^{-4}$
O	1 31 $\times 10^{-2}$	1 31 $\times 10^{-2}$	5 0 $\times 10^{-3}$	8 74$\times 10^{-3}$
Ne	8 43 $\times 10^{-3}$	8 43 $\times 10^{-3}$	8 43 $\times 10^{-3}$	5 62$\times 10^{-3}$
Na	4 883$\times 10^{-5}$	4 883$\times 10^{-5}$	4 883$\times 10^{-5}$	3 26$\times 10^{-5}$
Mg	6 50 $\times 10^{-4}$	6 50 $\times 10^{-4}$	6 50 $\times 10^{-4}$	4 34$\times 10^{-4}$
Al	4 55 $\times 10^{-5}$	4 55 $\times 10^{-5}$	4 55 $\times 10^{-5}$	3 04$\times 10^{-5}$
Si	1 19 $\times 10^{-3}$	1 19 $\times 10^{-3}$	1 19 $\times 10^{-3}$	7 94$\times 10^{-4}$
S	5 05 $\times 10^{-4}$	5 05 $\times 10^{-4}$	5 05 $\times 10^{-4}$	3 37$\times 10^{-4}$
Ca	6 03 $\times 10^{-5}$	6 03 $\times 10^{-5}$	6 03 $\times 10^{-5}$	4 03$\times 10^{-5}$
Fe	2 21 $\times 10^{-4}$	2 21 $\times 10^{-4}$	2 21 $\times 10^{-4}$	1 47$\times 10^{-4}$
Ni	5 08 $\times 10^{-5}$	5 08 $\times 10^{-5}$	5 08 $\times 10^{-5}$	3 39$\times 10^{-5}$

For example, the reduction of the C/N ratio will take place during a period of time related to the mean lives of the C^{12} and C^{13} nuclei. Actually, since the mean life of C^{13} is substantially shorter than the mean life of C^{12}, the value of the latter is the one that determines the rate of conversion. Since these mean lives are quite short compared to the mean life of N^{14} the reaction $N^{14}(p, \gamma)O^{15}$ proceeds only to an insignificant degree during the period of readjustment. In point of fact the difference between the C and N mean lives is accentuated by the comparatively low temperature that exists during the pre-main-sequence phase of evolution, since the reaction rate for N^{14} is somewhat more temperature-sensitive than the carbon reaction rates.

On the other hand, the readjustment of the O/N ratio must take place on a longer time scale. In fact, the mean life of O^{16} for the $O^{16}(p, \gamma)F^{17}$ reaction is more nearly like the mean life of hydrogen itself. Thus the readjustment of the O/N ratio takes place during an appreciable fraction of the life of the star on the main sequence.

III. DESCRIPTION OF RESULTS

The present discussion is concerned with the pre-main-sequence and main-sequence evolution of four models, each with a mass of 2.3 and chemical composition as given in Table 1.

The column for Sequence I is based essentially on the atmospheric values already described. The values for the species through oxygen affect the hydrogen thermonuclear reactions, the equation of state, and the opacity. In addition, neon affects the equation of state calculation. The values for the remaining species are needed to describe physical conditions in the stellar atmosphere. Certainly the structure of the atmosphere does not greatly affect the external boundary conditions for stars in this phase of evolution with these effective temperatures. Nonetheless the computer program demands these data and they are provided. It must be noted that not all elements are represented in the table. The choice of elements, as well as the values of their abundances, represents a compromise which attempts to describe the ionization properties of the heavy elements in an average way. The values for Sequence I (excluding H and He) are the concentrations by mass based on the number concentrations given by Aller (1961). The H concentration was set at 0.68 and the concentrations of the heavier elements are, in turn, based on the total value $Z = 0.03$. The values given for Sequences II and III differ from the values of Sequence I for reasons which are elaborated below. Sequence IV is similar to Sequence I but with $Z = 0.02$.

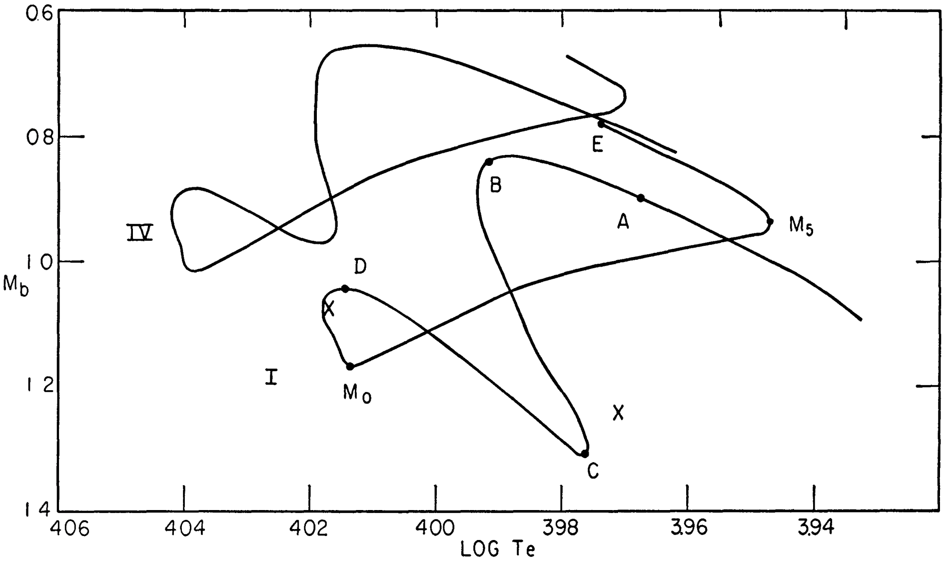

FIG. 1 —Evolutionary tracks in the (log T_e, M_b) plane for Sequences I and IV, showing the effect of a change in metal content Z. Points corresponding to epochs A, B, C, D, M_0, M_5, and E are shown by dots on the track for Sequence I. Crosses indicate the two positions of the star, Sirius, deduced from observations.

Figure 1 contains evolutionary tracks in the (log T_e, M_b) plane for Sequences I and IV. First let us consider Sequence I. The calculations were initiated using techniques described in Appendix E. From the starting point through points A, B, C, D, and up to the point M_0, the curve represents the pre-main-sequence evolutionary phases. Between point M_0 and point M_5 the curve gives the main-sequence development. A very short portion of the post-main-sequence phase is shown by the interval M_5 to E. Table 2 gives the values for several of the parameters of interest in describing the configuration, at the labeled points on the curve. The second column gives the values of the time in years referred to an arbitrary zero adopted for epoch M_0. Presumably this corresponds to a position on the so-called zero-age main sequence. The bolometric absolute magnitude and the effective temperature are given in the two following columns. The central temperature, density, and hydrogen concentration are in the next three columns. M_0 and M_5 correspond to epochs which were actually encountered in the time sequence set up by the computer and represent times for which an abrupt change in the evolutionary time scale occurs. The intermediate epochs M_1–M_4 divide the main sequence into five equal parts in terms of the central hydrogen concentration.

The novel feature of the track for Sequence I in Figure 1 is the dip at point *C*. An understanding of the phenomena producing this effect is aided by an examination of Figures 2, 3, and 4, in which various relevant quantities are plotted as a function of time. Before epoch *A* the configuration is essentially in gravitational contraction. Any input transients which affect the early shape of the curve (Fig. 1) could certainly be modified by starting the calculations further back in the contraction phase of the evolution. Figure 4, in which central values of the concentrations are plotted, indicates that the reactions proceed only slightly, but sufficiently to convert a small amount of C^{12} into C^{13} and N^{14}. In fact C^{13} is brought closer to equilibrium with C^{12}.

Between points *A* and *B* the thermonuclear tempo is greatly accelerated causing the fraction of the energy release due to reactions to increase from 6 to 49 per cent. The drop in luminosity between epochs *B* and *C* is the usual drop associated with the onset of nuclear-energy sources (Henyey, LeLevier, and Levée 1955). However, since it results from the conversion of C, it takes place on a more rapid time scale than is given by the earlier results. These use the whole cycle as driven by a single reaction rate, assuming by implication equilibrium concentrations. This rapid change is associated with an expansion of the inner half of the mass of the star and, therefore, with a considerable deposition of energy into the gravitational field by the work done. The behavior of the inner regions is shown graphically in Figure 6. The time variation of the radius for a number of mass points is plotted for the time interval within which the expansion takes place. In Figure 5 the variation of the luminosity $l(r)$ is given for an epoch intermediate between *B* and *C*, where $M_b = 1.07$. After an initial increase the curve drops to a minimum slightly before the half-mass point and then rises again ultimately to reach the constant value equal to the surface luminosity. The drop in l is the result of the deposition of gravitational energy. Some idea of its significance may be obtained by considering an approximate extrapolation as indicated by the dashed curve and considering the difference between it and the real variation shown by the solid curve. Obviously such a comparison is only approximate but it does give some idea of the large loss of luminosity to the star: roughly one third of the energy is reabsorbed in the form of work. Figure 3 describes the relationship between thermonuclear and gravitational energy production in the form of the ratio of nuclear to total energy output. The maximum which falls between *B* and *C* at the epoch for Figure 5 is not the result of the strong emergence of thermonuclear energy but rather of the large negative gravitational effect. The ultimate dominance of nuclear-

TABLE 2

EVOLUTION OF 2.3 $M_\odot$, SEQUENCE I

Model	Time (yr)	M_b	T_e(° K)	T_c(° K)	ρ_c(gm/cm³)	$(H^1)_c$
A	$-11\ 873\times10^{6}$	$+0\overset{\mathrm{m}}{.}90$	9284	$16\ 1\times10^{6}$	37 8	0 67995
B .	$-11\ 688\times10^{6}$	0 83	9732	$18\ 5\times10^{6}$	40 5	67989
C .	$-11\ 125\times10^{6}$	1 31	9452	$19\ 2\times10^{6}$	35 5	67947
D	$-10\ 343\times10^{6}$	1 05	10330	$20\ 9\times10^{6}$	52 3	67886
M_0	0	1 17	10334	$21\ 8\times10^{6}$	52 1	66998
M_1	$+128\ 28\ \times10^{6}$	1 11	10032	$22\ 1\times10^{6}$	51 9	.54635
M_2	$234\ 86\ \times10^{6}$	1 06	9742	$22\ 5\times10^{6}$	54 0	42272
M_3	$321\ 72\ \times10^{6}$	1 01	9431	$23\ 1\times10^{6}$	57 7	.29909
M_4	$395\ 27\ \times10^{6}$	0 97	9089	$24\ 0\times10^{6}$	63 5	17546
M_5	$445\ 11\ \times10^{6}$	0 94	8848	$25\ 7\times10^{6}$	81 2	05183
E	$+456\ 97\ \times10^{6}$	+0 77	9406	$29\ 3\times10^{6}$	129 9	0 00363

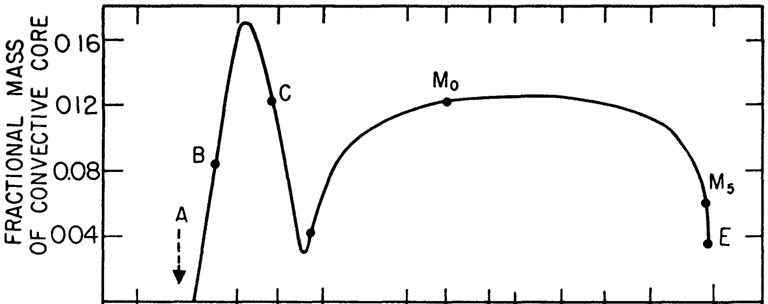

Fig 2

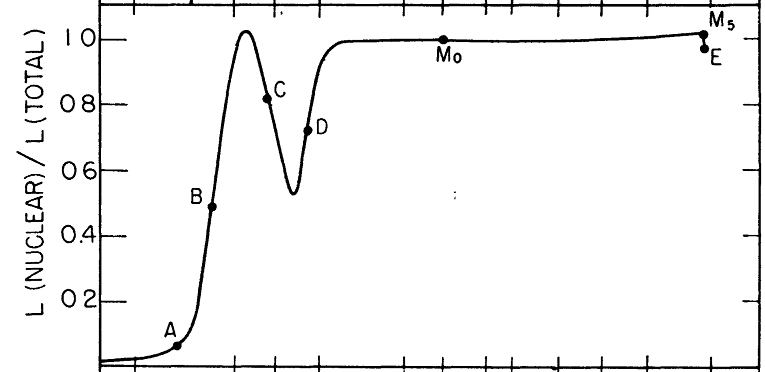

Fig 3

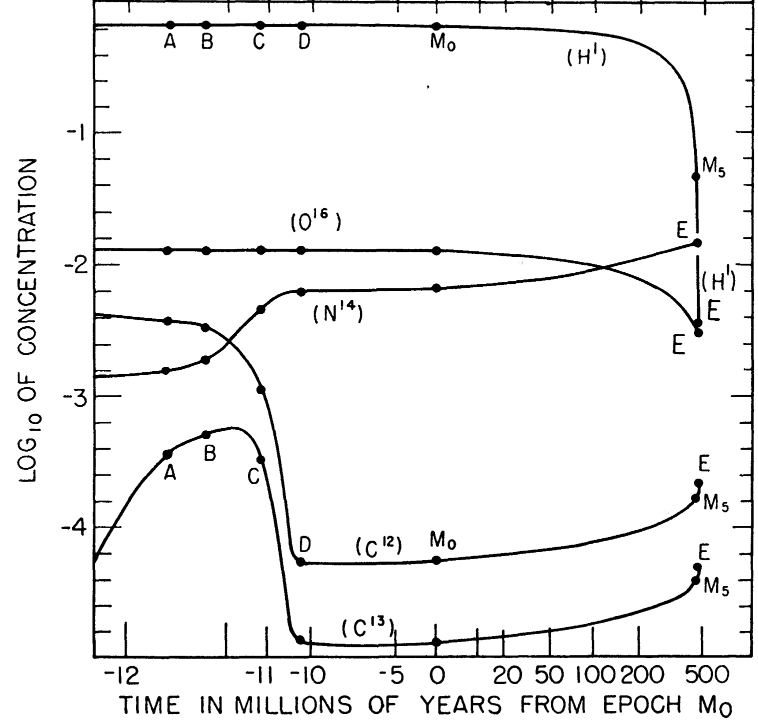

Fig 4

Fig. 2.—The fraction of the stellar mass contained in the convective core as a function of time for Sequence I. Salient epochs in the evolution are indicated by dots. The time scale in the pre–main-sequence phase is greatly expanded relative to the main-sequence phase.

Fig. 3.—The ratio of energy output from nuclear reactions to total luminosity as a function of time for Sequence I. The time scale is identical with that of Fig. 2.

Fig. 4.—Central composition as a function of time for Sequence I. The curves show the concentrations, in grams per gram of stellar matter, of H^1, C^{12}, C^{13}, N^{14}, and O^{16}. Salient epochs are marked by dots.

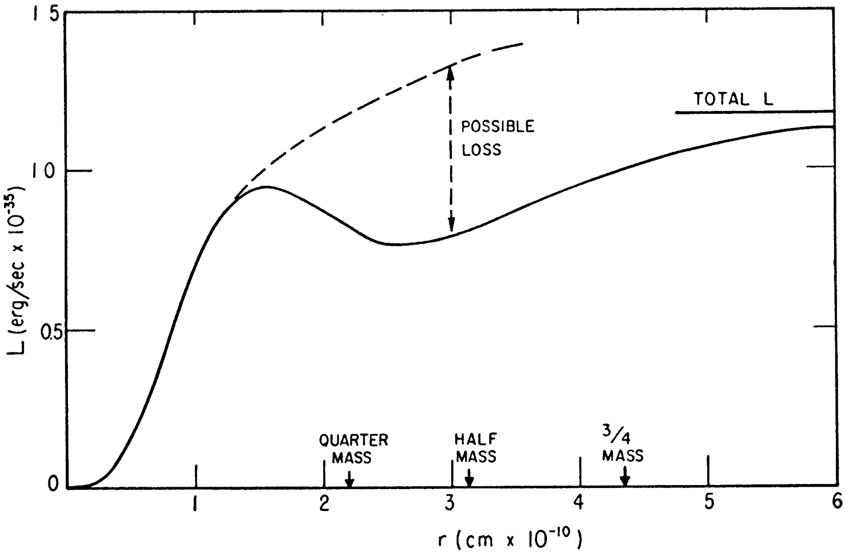

FIG. 5.—The luminosity $l(r)$ at an epoch intermediate between B and C for Sequence I The solid curve shows the true variation of l The dashed curve shows roughly how l would vary if no energy were lost as work against the gravitational field. The surface value of the luminosity, L, is indicated at the right, and the values of r are shown for which $m(r) = \frac{1}{4}M$, $\frac{1}{2}M$, and $\frac{3}{4}M$.

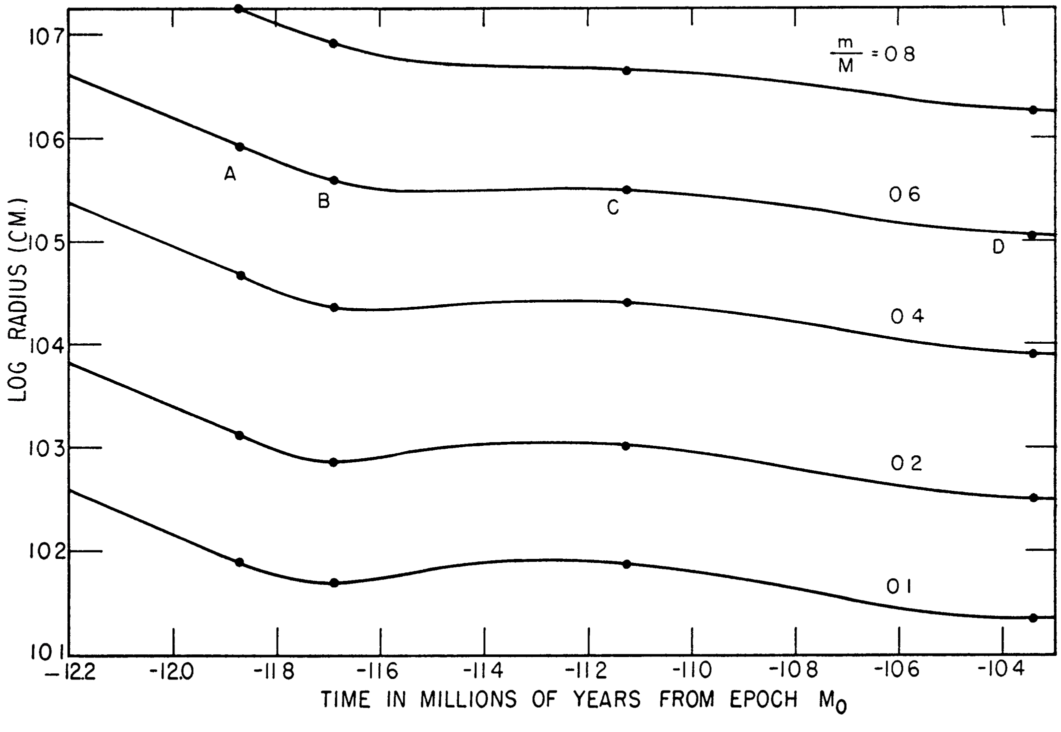

FIG. 6.—Variations in log r as a function of time for the mass points $m/M = 0.8, 0.6, 0.4, 0.2$, and 0.1 of Sequence I. The time interval represented is that during which the initial adjustment of the model takes place. Where the curves are all parallel, the model is undergoing homologous contraction. Epochs A, B, C, and D are shown as dots.

energy sources occurs at somewhat later epochs for which the curve levels off at values near unity. The explanation for this phenomenon must be found in the mild but sudden emergence of the C reactions which cause the central regions to expand slightly, thereby producing an amplified uplift of the intermediate layers. This expansion does not reach the outermost layers of the star, and the total radius continues to decrease. The density decrease in the neighborhood of epoch C is apparent in Table 2. After epoch C the importance of the carbon conversion becomes less and less, resulting in a disappearance of the internal luminosity drop at an epoch between C and D. The approach to epoch D is mainly through gravitational contraction, gradually modified by the emergence of the full CNO cycle. At this later epoch, according to Figure 4, the C and N isotopes are present with very nearly equilibrium concentrations. After epoch D the nuclear-energy sources become increasingly dominant and cause the inner regions of the star again to grow in size until the zero-age main-sequence epoch, M_0, is reached. The decrease in density now takes place on a greatly extended time scale and leads to only a negligible loss of energy back to the gravitational field.

Up to epoch M_0 the modification of the O^{16} abundance has been entirely negligible. The importance of the oxygen branch of the CNO bi-cycle is felt only in the main-sequence phase, between epochs M_0 and M_5. During this time the O^{16} abundance gradually drops while the N^{14} abundance increases in a complementary way. Moreover the C^{12} and C^{13} abundances increase to maintain equilibrium ratios with N^{14}.

The extent of the convective core (Fig. 2) varies in an interesting manner during the changes just described. Shortly after epoch A the convective core suddenly makes its appearance. Its mass achieves a maximum value at an epoch practically identical with that of the first maximum in Figure 3. It then recedes to a minimum size just before epoch D and slightly after the epoch for the minimum in Figure 3. Thereafter it again expands, achieving a maximum mass slightly later than M_0. From then on it once more gradually recedes, leaving behind a chemical gradient in which the H and He abundances vary complementarily. It should be noted here that the calculations show no convective envelope at any point in the model sequences, a result which is to be expected for stars of high surface temperature.

In the preceding discussion reference to the p-p reactions has been omitted. A detailed examination of the printed output from the computer shows that these reactions play a completely negligible role during the dominance of the purely C reactions. Only after the N^{14} reaction has emerged does the p-p chain contribute to any extent. However, it never competes, even locally, with the CNO cycle, since in the regions of relatively low temperature only the C^{12} to N^{14} step is important. Thus the expected dominance of the p-p reactions at low temperatures is vitiated.

Returning to Figure 1 we note that for $Z = 0.02$ (Sequence IV) the complex of phenomena resulting from the C to N pre-main-sequence conversion takes place on a reduced scale as compared with the case $Z = 0.03$ just discussed. The explanation for this behavior is found in the higher temperature governing the evolutionary changes in the low-Z case, as compared with the other. The lowering of Z causes an increase in luminosity, and hence in central temperature (Henyey *et al.* 1955). In order to verify that the increased temperature does, in fact, modify the C to N transition, we examine the relative rate of emergence of the $N^{14}(p, \gamma)O^{15}$ reaction in the two cases. Between epochs B and C, for Sequence I, the C^{12} reaction rate increases by a factor of 1.85 while the N^{14} reaction rate increases by a very slightly larger factor of 1.99. For Sequence IV, the corresponding factors are 4.92 and 5.93, respectively. Thus it appears that for a lower Z the N^{14} reaction emerges earlier relative to the C^{12} reaction, and the separation of the two parts of the CN cycle is less distinct.

Sequence II differs from Sequence I in that the C^{12} and N^{14} abundances alone have been modified to values corresponding to very nearly equilibrium concentrations. Figure 7 shows the influence of this modification on evolutionary tracks. The early pre-main-sequence and main-sequence phases are practically identical and, as may be expected, the effects originating from the C to N conversion are absent.

Sequence III shows the result of modifying the O/N ratio. Its evolutionary track is compared with that of Sequence II in Figure 8. The early pre-main-sequence evolution is again identical in the two cases. The two tracks very nearly come together in the late main-sequence phase. This result confirms our expectation that the excess O^{16} is only gradually converted to CN isotopes. The incomplete merging of the two tracks results from the fact that in the two cases O and N were changed by equal amounts. Since the conversion of a given amount of O^{16} produces only $\frac{14}{16}$ as much N^{14} by weight it

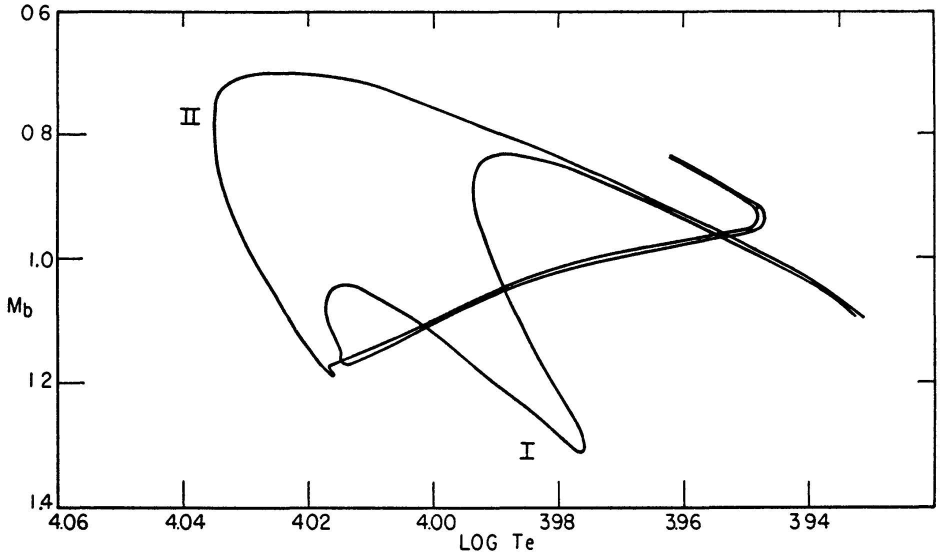

FIG. 7.—Evolutionary tracks for Sequences I and II, showing the effect of altering the C^{12}/N^{14} ratio from non-equilibrium to equilibrium value. $Z = 0.03$.

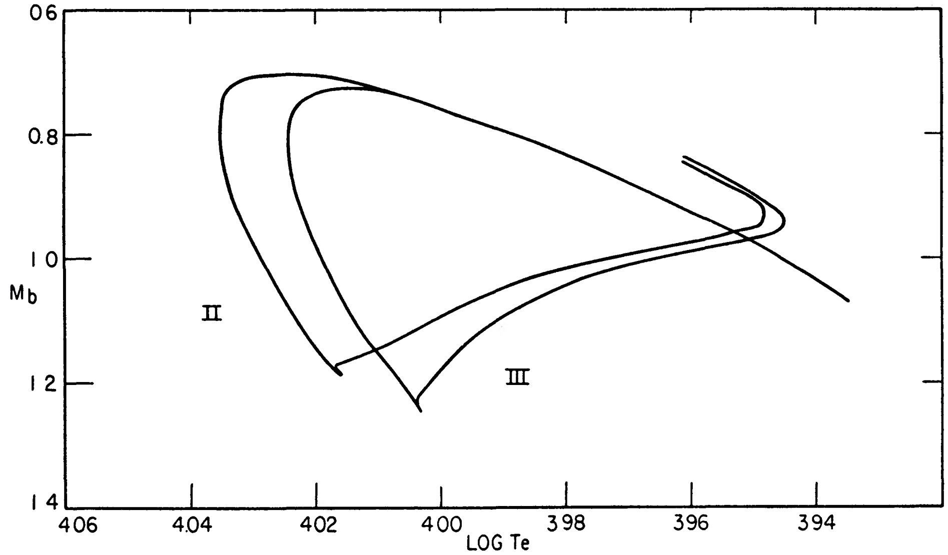

FIG. 8.—Evolutionary tracks for Sequences II and III, showing the effects of altering the O/N ratio. For both II and III, $Z = 0.03$ and C^{12}/N^{14} has its equilibrium value.

1965ApJ...141.1019B

might have been slightly preferable to prepare Sequence III with this factor in mind. The difference between the late pre-main-sequence tracks is related to the fact that Sequence III now starts with a relative deficiency of the carbon isotopes.

In Tables 4A, 4B, and 4C, detailed stellar models are given for $t = -5.46 \times 10^6$, $+330 \times 10^6$, and $+457 \times 10^6$ years, respectively, corresponding closely to epochs M_0, M_3, and E of Sequence I. The model in Table 4B was chosen so that its age agreed as closely as possible with the value of 300 million years tentatively assumed for Sirius. The model in Table 4A is roughly the zero-age main-sequence model, while that in Table 4C is nearly depleted of hydrogen at the center and thus represents the end of the main-sequence phase. In all three tables, the first column gives the Lagrangian coordinate ξ.

TABLE 3

MASS TABLE

ξ	$m(\xi)/M$	$m'(\xi)/M$
0 .	0	0
0 04	0 001875588	0 1394598
0 08	0 01443948	0 5231362
0 12	0 04576924	1 059115
0 16	0 09961468	1 628863
0 20	0 1750430	2 122163
0 24	0 2673317	2 462775
0 28	0 3695784	2 618245
0 32	0 4744017	2 595397
0 36	0 5752720	2 427588
0 40	0 6672832	2 160359
0 44	0 7473922	1 839736
0 48	0 8142772	1 504899
0 52	0 8679871	1 184946
0 56	0 9095249	0 8986014
0 60	0 9404564	0 6556184
0 64	0 9625928	0 4588703
0 68	0 9777589	0 3064889
0 72	0 9876406	0 1937103
0 76	0 9937008	0 1143107
0 80	0 9971416	0 06163132
0 84	0 9989017	0 02925160
0 88	0 9996748	0 01138928
0 92	0 9999400	0 003102245
0 96	0 9999965	0 0003552120
1 00	1 000000	0 0

The relationship between ξ and the mass distribution is given in Table 3. The second column of Tables 4A, 4B, and 4C gives the radial distance r in centimeters; the third column, the density in gm/cm^3; the fourth column, the temperature in °K; the fifth column, the pressure in dyne/cm^2; the sixth column, the luminosity in erg/sec; and the seventh through the twelfth columns, the concentrations of the species shown in grams per gram of mixture. An integer in parentheses gives the power of 10 by which the number is to be multiplied; e.g., $2.6(-6)$ means 2.6×10^{-6}.

IV. COMPARISON WITH OBSERVATIONS

For purposes of comparing our calculated models with Sirius itself we have used the relation among effective temperature, $B - V$ color index, and bolometric correction given in Table 7 of Harris (1963), slightly smoothed. The observed value of $B - V = +0.01$ for Sirius, given by Johnson and Morgan (1953), corresponds, in the smoothed Harris table, to $T_e = 10400°$. However, a fundamental determination of the effective

TABLE 4A

MODEL AT t = -5 46 × 10^{6} YEARS

16	ξ	r(ξ)	ρ(ξ)	T(ξ)	P(ξ)	l(ξ)	H^1	He^3	C^{12}	C^{13}	N^{14}	O
(-2)	00	0 000	5.221 (1)	2 178 (7)	1.501 (17)	0 000	0.67470	2.6 (-6)	5 55 (-5)	1.32 (-5)	6 50 (-3)	1.29
"	04	3 417 (9)	5.128 (1)	2.152 (7)	1.458 (17)	6.455 (33)	"	"	"	"	"	
"	08	6 819 (9)	4.862 (1)	2.078 (7)	1.334 (17)	3.518 (34)	"	"	"	"	"	
"	12	1.019 (10)	4.452 (1)	1 961 (7)	1 152 (17)	6.771 (34)	"	"	"	"	"	
"	16	1 353 (10)	3 939 (1)	1.809 (7)	9.402 (16)	8.540 (34)	"	"	"	"	"	
(-2)	17014*	1.436 (10)	3 792 (1)	1 766 (7)	8 847 (16)	8 784 (34)	.67645	8.9 (-6)	4 29 (-5)	1 03 (-5)	6.44 (-3)	1 30
(-2)	20	1 682 (10)	3.341 (1)	1 641 (7)	7 254 (16)	9 443 (34)	.67886	1 7 (-5)	1.18 (-4)	3.37 (-5)	6.24 (-3)	1 31
"	24	2 011 (10)	2 699 (1)	1 484 (7)	5.299 (16)	1.024 (35)	67948	3.8 (-5)	2.05 (-3)	5.48 (-4)	3.43 (-3)	
"	28	2.344 (10)	2 081 (1)	1.335 (7)	3.674 (16)	1 063 (35)	.67986	6.6 (-5)	3.86 (-3)	3.37 (-4)	1 55 (-3)	
"	.32	2 683 (10)	1.533 (1)	1.196 (7)	2 424 (16)	1.071 (35)	67995	4.7 (-5)	4.17 (-3)	8 76 (-5)	1.45 (-3)	
"	36	3.033 (10)	1 082 (1)	1 068 (7)	1.528 (16)	1.073 (35)	.67998	2.1 (-5)	4 20 (-3)	5 66 (-5)	"	
"	40	3.398 (10)	7 345 (0)	9 502 (6)	9.220 (15)	1.074 (35)	.67999	8.3 (-6)	"	5 42 (-5)	"	
"	44	3.779 (10)	4.811 (0)	8.412 (6)	5 344 (15)	"	68000	3.0 (-6)	"	5.40 (-5)	"	
"	.48	4 181 (10)	3.049 (0)	7 406 (6)	2.982 (15)	"	"	1.0 (-6)	"	"	"	
"	52	4 605 (10)	1.874 (0)	6 480 (6)	1 603 (15)	"	"	3.0 (-7)	"	"	"	
"	56	5 052 (10)	1.119 (0)	5 627 (6)	8.313 (14)	"	"	Negligible	"	"	"	
"	60	5 523 (10)	6.496 (-1)	4 841 (6)	4.151 (14)	"	"	"	"	"	"	
"	64	6 017 (10)	3.662 (-1)	4 118 (6)	1.990 (14)	"	"	"	"	"	"	
"	.68	6 532 (10)	1 999 (-1)	3 452 (6)	9 109 (13)	"	"	"	"	"	"	
"	.72	7 064 (10)	1.050 (-1)	2.841 (6)	3 938 (13)	"	"	"	"	"	"	
"	76	7 609 (10)	5.237 (-2)	2 286 (6)	1.580 (13)	"	"	"	"	"	"	
"	80	8 162 (10)	2 426 (-2)	1 787 (6)	5.719 (12)	"	"	"	"	"	"	
"	84	8 720 (10)	1 003 (-2)	1 343 (6)	1.777 (12)	"	"	0.0	"	"	"	
"	88	9 282 (10)	3 424 (-3)	9 507 (5)	4 295 (11)	"	"	0 0	"	"	"	
"	.92	9 851 (10)	8.077 (-4)	6.109 (5)	6 511 (10)	"	"	0 0	"	"	"	
"	96	1.046 (11)	6 877 (-5)	3.378 (5)	3 080 (9)	"	"	0 0	"	"	"	
"	00	1.149 (11)	0 000		0.000	"	"	0.0	"	"	"	

* Denotes outer boundary of convective core

TABLE 4B

MODEL AT t = +3.30 × 10^8 YEARS

O^{16}	ξ	r(ξ)	ρ(ξ)	T(ξ)	P(ξ)	l(ξ)	H^1	He^3	C^{12}	C^{13}	N^{14}	
31 (-3)	0.00	0.000	5.812 (1)	2.315 (7)	1 238 (17)	0 000	0.28624	1.2 (-7)	1 24 (-4)	2.94 (-5)	1.30 (-2)	5.
"	.04	3.302 (9)	5.668 (1)	2.277 (7)	1 187 (17)	1 406 (34)	"	"	"	"	"	
"	.08	6.618 (9)	5.254 (1)	2.167 (7)	1.047 (17)	6.652 (34)	"	"	"	"	"	
"	.12	9.970 (9)	4.618 (1)	1 992 (7)	8.452 (16)	1.073 (35)	"	"	"	"	"	
"	.15531*	1.299 (10)	3.923 (1)	1.790 (7)	6.448 (16)	1.190 (35)	"	"	"	"	"	
49 (-3)	.16	1.340 (10)	3.764 (1)	1.760 (7)	6.192 (16)	1.188 (35)	.30248	4.6 (-7)	1 13 (-4)	2.69 (-5)	1.29 (-2)	5.
40 (-3)	.17	1.440 (10)	2.929 (1)	1 699 (7)	5 640 (16)	1.200 (35)	.49593	5.8 (-6)	6.24 (-5)	1 49 (-5)	1.04 (-2)	8
28 (-2)	18	1.552 (10)	2 423 (1)	1 639 (7)	5.124 (16)	1.210 (35)	.64727	1.6 (-5)	3 69 (-5)	8.83 (-6)	6.62 (-3)	1.
30 (-2)	.20	1 785 (10)	2.119 (1)	1 531 (7)	4.226 (16)	1.225 (35)	.66040	2.9 (-5)	3 13 (-5)	7.51 (-6)	6.44 (-3)	1.
31 (-2)	.24	2.238 (10)	1.600 (1)	1.347 (7)	2.832 (16)	1.241 (35)	.67180	7.5 (-5)	2.46 (-5)	5.96 (-6)	6.38 (-3)	1.
31 (-2)	.28	2.689 (10)	1.170 (1)	1.191 (7)	1.836 (16)	1.247 (35)	.67625	1.7 (-4)	6 03 (-4)	1.85 (-4)	5.50 (-3)	1.
"	.32	3 147 (10)	8 242 (0)	1.053 (7)	1.146 (16)	1.249 (35)	.67853	3.5 (-4)	3 52 (-3)	5.19 (-4)	1.75 (-3)	
"	.36	3 621 (10)	5 602 (0)	9.302 (6)	6.881 (15)	"	.67932	5.2 (-4)	4 15 (-3)	1 06 (-4)	1.46 (-3)	
"	40	4.115 (10)	3 681 (0)	8.189 (6)	3.980 (15)	"	.67972	2.8 (-4)	4.20 (-3)	5.71 (-5)	1.45 (-3)	
"	.44	4.635 (10)	2.343 (0)	7 181 (6)	2.222 (15)	1.248 (35)	.67990	1.0 (-4)	"	5.41 (-5)	"	
"	48	5.184 (10)	1.449 (0)	6 266 (6)	1.199 (15)	"	.67997	3.2 (-5)	"	5.40 (-5)	"	
"	52	5 764 (10)	8.728 (-1)	5.433 (6)	6.260 (14)	"	.67999	9 3 (-6)	"	"	"	
"	56	6 377 (10)	5.130 (-1)	4.674 (6)	3.166 (14)	"	.68000	2 4 (-6)	"	"	"	
"	60	7.021 (10)	2.944 (-1)	3.982 (6)	1.548 (14)	"	"	5.6 (-7)	"	"	"	
"	.64	7.694 (10)	1.648 (-1)	3.353 (6)	7.297 (13)	"	"	1.1 (-7)	"	"	"	
"	.68	8.392 (10)	8.966 (-2)	2.783 (6)	3.294 (13)	"	"	Negligible	"	"	"	
"	.72	9.109 (10)	4 698 (-2)	2.271 (6)	1 408 (13)	1.247 (35)	"	"	"	"	"	
"	76	9.840 (10)	2 338 (-2)	1.815 (6)	5.602 (12)	"	"	"	"	"	"	
"	80	1.058 (11)	1.079 (-2)	1.412 (6)	2.012 (12)	"	"	"	"	"	"	
"	.84	1.133 (11)	4.437 (-3)	1.060 (6)	6.207 (11)	"	"	0.0	"	"	"	
"	88	1.208 (11)	1.498 (-3)	7.526 (5)	1.488 (11)	"	"	0.0	"	"	"	
"	92	1.286 (11)	3.435 (-4)	4.918 (5)	2.232 (10)	"	"	0.0	"	"	"	
"	.96	1.371 (11)	2.938 (-5)	2.680 (5)	1.046 (9)	"	"	0.0	"	"	"	
"	1 00	1.500 (11)	0.000		0.000	"	"	0.0	"	"	"	

* Denotes outer boundary of convective core

TABLE 4C

MODEL AT t = +4.57 × 10^{8} YEARS

O^{16}	ξ	r(ξ)	ρ(ξ)	T(ξ)	P(ξ)	l(ξ)	H^1	He^3	C^{12}	C^{13}	N^{14}	
08 (-3)	0.00	0.000	1.299 (2)	2.926 (7)	2.391 (17)	0.000	0.00362	Negligible	2.15 (-4)	5.06 (-5)	1.49 (-2)	3.
"	.04	2.532 (9)	1.250 (2)	2.855 (7)	2.245 (17)	1.950 (34)	"	"	"	"	"	
"	08	5.118 (9)	1.111 (2)	2.644 (7)	1.846 (17)	7.670 (34)	"	"	"	"	"	
"	.11007*	7.154 (9)	9.550 (1)	2.397 (7)	1.437 (17)	9 951 (34)	"	"	"	"	"	
10 (-3)	.12	7.834 (9)	8.939 (1)	2.305 (7)	1.299 (17)	1.047 (35)	.00626	"	1 87 (-4)	4.42 (-5)	"	3
69 (-3)	.14	9.356 (9)	6.691 (1)	2.120 (7)	1.015 (17)	1.196 (35)	.08879	"	1.32 (-4)	3.13 (-5)	1.44 (-2)	3.
45 (-3)	.16	1.131 (10)	4.276 (1)	1.928 (7)	7.638 (16)	1.372 (35)	.29369	3.6 (-7)	9.89 (-5)	2 35 (-5)	1 30 (-2)	5.
39 (-3)	.17	1.252 (10)	3.198 (1)	1.836 (7)	6.608 (16)	1.414 (35)	48838	2.4 (-6)	7 22 (-5)	1.72 (-5)	1.04 (-2)	8.
28 (-2)	.18	1.387 (10)	2.559 (1)	1.751 (7)	5.757 (16)	1.440 (35)	.64145	8.6 (-6)	4.14 (-5)	9.85 (-6)	6.63 (-3)	1.
30 (-2)	.20	1.658 (10)	2.133 (1)	1.608 (7)	4.460 (16)	1.469 (35)	.65732	2.1 (-5)	3.21 (-5)	7 58 (-6)	6.44 (-3)	1.
31 (-2)	.24	2.172 (10)	1.512 (1)	1.385 (7)	2.751 (16)	1.500 (35)	.67072	8.0 (-5)	2 32 (-5)	5.65 (-6)	6.38 (-3)	1
"	.28	2.676 (10)	1.058 (1)	1.208 (7)	1.684 (16)	1.518 (35)	.67582	2.4 (-4)	5.72 (-4)	1.76 (-4)	5.55 (-3)	
"	.32	3.187 (10)	7.196 (0)	1.058 (7)	1.005 (16)	1.528 (35)	.67834	4.5 (-4)	3.51 (-3)	5.23 (-4)	1.75 (-3)	
"	.36	3.716 (10)	4.749 (0)	9.264 (6)	5.810 (15)	1.534 (35)	.67924	5.9 (-4)	4.15 (-3)	1.07 (-4)	1.46 (-3)	
"	.40	4.271 (10)	3.042 (0)	8.094 (6)	3.252 (15)	1.539 (35)	.67969	3.1 (-4)	4.20 (-3)	5 70 (-5)	1.45 (-3)	
"	.44	4.856 (10)	1.893 (0)	7.049 (6)	1.763 (15)	1.542 (35)	.67989	1.1 (-4)	"	5.41 (-5)	"	
"	.48	5.475 (10)	1.148 (0)	6.111 (6)	9.269 (14)	1.544 (35)	.67997	3.5 (-5)	"	5 40 (-5)	"	
"	.52	6.133 (10)	6.799 (-1)	5.267 (6)	4.730 (14)	1.545 (35)	.67999	1.0 (-5)	"	"	"	
"	.56	6.828 (10)	3 938 (-1)	4.504 (6)	2.343 (14)	1.546 (35)	.68000	2.6 (-6)	"	"	"	
"	.60	7.560 (10)	2.232 (-1)	3.816 (6)	1.125 (14)	1.547 (35)	"	5.9 (-7)	"	"	"	
"	64	8.326 (10)	1.237 (-1)	3.195 (6)	5 222 (13)	"	"	1.2 (-7)	"	"	"	
"	.68	9.120 (10)	6.671 (-2)	2.638 (6)	2 325 (13)	"	"	Negligible	"	"	"	
"	.72	9.935 (10)	3.470 (-2)	2.143 (6)	9.824 (12)	"	"	"	"	"	"	
"	.76	1.077 (11)	1.715 (-2)	1.707 (6)	3.866 (12)	"	"	"	"	"	"	
"	.80	1.161 (11)	7.862 (-3)	1.325 (6)	1.376 (12)	"	"	"	"	"	"	
"	.84	1.246 (11)	3.211 (-3)	9.923 (5)	4.208 (11)	"	"	0.0	"	"	"	
"	.88	1.333 (11)	1.074 (-3)	7.046 (5)	9.998 (10)	"	"	0.0	"	"	"	
"	.92	1.422 (11)	2.430 (-4)	4.624 (5)	1.486 (10)	"	"	0.0	"	"	"	
"	.96	1.521 (11)	2.082 (-5)	2.485 (5)	6.881 (8)	"	"	0.0	"	"	"	
"	1.00	1.666 (11)	0.000		0.000	"	"	0.0	"	"	"	

* Denotes outer boundary of convective core.

temperature, based on observation of the angular diameter of Sirius, produces $T_e = 9350 \pm 400°$, corresponding in the Harris table to $B - V = +0.08$. This value and the resulting discrepancy are discussed by Popper (1959), who emphasizes the uncertainty in our knowledge of the effective temperatures of early A stars. If we adopt a visual apparent magnitude of $V = -1.43$ and a parallax of 0".367 (Harris, Strand, and Worley 1963), these two values of T_e give, respectively, B.C. = -0.38 and -0.21, and $M_b = +1.07$ and $+1.24$. These two deduced positions of Sirius in the ($\log T_e, M_b$) plane are shown in Figure 1, with the calculated tracks.

The mass adopted in the calculation, $M = 2.3\ M_\odot$, was chosen on the basis of the value

$$\log (M/M_\odot) = +0.36$$

for Sirius A, given by van de Kamp (1958). A newer value of $\log (M/M_\odot) = +0.33$, given by Harris *et al.* (1963) is based on observations of the orbit by van den Bos (1960). Close agreement of the theoretical curve for $Z = 0.03$ can be obtained with the observational point at $T_e = 9350°$ if the theoretical curve is moved downward by 0.2 mag. and to the right by 0.010 in $B - V$. Taking into account the fact that the luminosity varies approximately as the fourth power of the mass near $\log T_e = 4.0$, the shifted curve would correspond to a mass intermediate between the two observed values noted above, and would run through the observed point at an age of 3×10^8 years from point M_0. Such an age is consistent with the observational value of the age of the Ursa Major Stream estimated by von Hoerner (1957). It is also consistent with Eggen's (1960) observations, which suggest that the Sirius group is younger than the Hyades group, whose age is estimated by Henyey *et al.* (1959) as 5×10^8 years.

Since the adopted mass represents the higher of the two observed masses of Sirius, the second observational point, at $T_e = 10400°$, cannot be fitted at a reasonable age to the theoretical curve for $Z = 0.03$. However, the curve for $Z = 0.02$, adjusted for a slightly smaller mass, would run through this point at an age somewhat less than 3×10^8 years. The fit to the curve for $Z = 0.03$ seems to be the more reasonable one. All in all, the agreement between theoretical and observed points cannot be considered unsatisfactory when one takes into account the uncertainties in the observational data, in the choice of chemical composition to be used in the calculation, and in the theory, especially the opacity values used.

The results of these calculations suggest that the initial concentrations of the different chemical species may have a very definite, if transient, effect upon the pre-main-sequence evolution and internal structure of stars. It would be extremely interesting if any observable manifestation of these effects could be discovered since it could be used to obtain information concerning the concentrations of carbon and nitrogen.

This research was supported by the Air Force Office of Scientific Research Grant AF-AFOSR-171-63. The authors express their appreciation to Dr. Arthur Cox for providing the Los Alamos opacity-code and opacity data in advance of publication.

APPENDIX A

EQUATION OF STATE

The evaluation of the pressure and internal energy as functions of the temperature, density, and composition must make allowance for a considerable range of physical conditions. The computing program must be able to represent the outer envelope of the Sun as well as the center of a red giant. The formulae given in the literature for different physical effects are actually conflicting in transition regimes and must therefore be modified heuristically. Approximations are necessary since in the strictest sense the theory of state variables is not completely worked out in all its aspects.

In addition to ideal gas conditions and radiative contributions we allow for incomplete ionization, for pressure effects, and for degeneracy including relativistic modifications. We omit all of the details of the compiled program but give here the principal approximations. Basically the technique is to iterate the electron density N_e, since if it is known all quantities may be derived from it (as well as the electron density itself!) by means of straightforward algorithms. Complications are present only if the simple expression $(1 + X)/2$, for the molar electron concentration is inadequate.

Incomplete ionization is handled by Saha's equation for hydrogen and helium with a rough allowance for the intermediately abundant elements C, N, O, and Ne. Generally these either are present in low concentration or are completely ionized (e.g., C^{12} in the core of an evolved star). Thus we may need only an approximate estimate of the incompleteness of their ionization to achieve a considerably higher over-all accuracy.

The level of ionization of the gas is determined principally by the Fermi energy (chemical potential per electron). In our work the number of free electrons released by C, N, O, and Ne are computed from the interpolation formula

$$\zeta = \begin{cases} Z \dfrac{(-\mu)}{a + (-\mu)}, & \mu < 0 \\ 0 \quad , & \mu > 0 \end{cases} \tag{A1}$$

where μ is the Fermi energy, Z the atomic number, ζ the free electrons per nucleus, and a is a constant characterizing the species in question. The justification of this approximate expression is based on two considerations. In the first place the ionization potential is a fairly smooth function of the stage of ionization (number of free electrons per ion) for highly ionized states. On the other hand the degree of ionization depends principally on what might be termed the principle of the dominant ionization level. This is determined by the order-of-magnitude condition on the ionization potential χ:

$$\chi \sim (-\mu) . \tag{A2}$$

Using these rough concepts one may expect some relation such as formula (A1). The particular form used proves adequate for our purposes, which require no more than an accuracy of 10 per cent for a species that altogether provides only 1 or 2 per cent of the free electrons. A single species may in special cases give substantially larger errors ($\sim$50 per cent), but the composite result averages well. The formula is correct in the limit of very high temperatures or low densities, $\mu \longrightarrow -\infty$. The values of the constant a are as follows:

C, 80 eV; N, 80 eV; O, 102 eV; Ne, 178 eV .

The calculation requires a relation between the temperature and density on the one hand and the Fermi energy on the other. In the absence of degeneracy we have that

$$e^{\mu/kT} = G \equiv \frac{h^3}{2(2\pi mkT)^{3/2}} N_e . \tag{A3}$$

Here G is defined by the extreme right-hand member of this equation. In the presence of degeneracy the relation is given by the Fermi function solved for $\mu = xkT$:

$$G = \frac{2}{\sqrt{\pi}} \int_0^\infty \frac{y^{1/2} dy}{e^{y-x} + 1} , \tag{A4}$$

which is valid only in the non-relativistic limit. An interpolation expression which serves our purpose is the following:

$$e^x \equiv e^{\mu/kT} = G + \frac{G^2}{4.45 + 2.257G + G^2} \exp\left[\left(\frac{3\sqrt{\pi}}{4} G\right)^{2/3}\right] . \tag{A5}$$

This formula is precise in the two limits of negligible and of extreme degeneracy. Its precision is shown in Table A1, which was calculated by determining G from x, using the rigorous tabulation given by McDougall and Stoner (1938) and then recomputing e^x from the approximation.

The influence of pressure ionization is estimated in the manner of Elste and Jugaku (1957) for hydrogen and helium. The procedure for C, N, O, and Ne is to modify the Fermi energy before substituting in equation (A3).

After an acceptable value of the electron density has been obtained, the value of the electron pressure, and hence the total pressure, as well as the internal energy follow readily.

For a non-degenerate gas

$$P_e = N_e kT , \qquad E_e = \tfrac{3}{2}\frac{P_e}{\rho} . \tag{A6}$$

To these must be added contributions for heavy particles, treated as non-degenerate, and for radiation. In addition, ionization terms which are calculated from the ionization equilibria must be added to the internal energy.

TABLE A1

x	Relative Error in e^x	Relative Error in H
$-\infty$	0	0
-4	−0 0063	−0 00005
0	+ 0032	− 0002
4	− 0260	− 0058
8	− 0250	− 0142
12	− 0041	− 0174
16	+ 0035	− 0155
20	−0 0095	−0 0110
∞	0	0

With the advent of degeneracy these equations for P_e and E_e must be corrected for its effect. Using the McDougall-Stoner (1938) tables we have devised the following correction factor whose precision is given in the third column of Table A1.

$$H = \frac{1}{1 + 0.000039277G^2} + \frac{0.176777G}{(1 + 0.04885G)^{1/3}} . \tag{A7}$$

This quantity must multiply the ideal gas representations of both P_e and E_e:

$$P_e = N_e kTH \quad \text{and} \quad E_e = \frac{3P_e}{2\rho} . \tag{A8}$$

Finally we must consider relativistic effects. Again correction factors will serve, one for each of the two quantities. Let x represent the measure of relativistic effects (Chandrasekhar 1939) according to the expression

$$N_e = \frac{8\pi m^3 c^3}{3h^3} x^3 . \tag{A9}$$

The adopted procedure is devised to be applicable when temperature effects are very small. The correction factor for P_e is then

$$1/K = 5f(x)/8x^5 , \tag{A10}$$

while the factor for E_e is

$$1/K' = 5g(x)/12x^5 , \tag{A11}$$

where $f(x)$ and $g(x)$ are given by Chandrasekhar. It is a remarkable fact that $2K' \cong 1 + K$ to a high order of precision. Moreover the approximate expression

$$K(x) = 0.0864 + 0.9136(1 + 0.7567x^2)^{1/2} \tag{A12}$$

serves our needs adequately.

The final formulae become

$$P_e = N_e kTH/K\,, \tag{A13}$$

$$E_e = 3N_e kTH/\rho(1 + K)\,. \tag{A14}$$

The effects of H and K are included only when they are needed since they are both unity over a very large range of physical conditions. In fact all complications are introduced only on the basis of reasonable criteria of significance.

APPENDIX B

OPACITY

The radiative absorption coefficient which is used in our calculations is an adaptation of the formulas used by Henyey, LeLevier, and Levée[2] (1959). They used an interpolation expression fitted to the opacity table of Keller and Meyerott (1955) and included components due to hydrogen, helium, heavy elements, and electron scattering. Our equations have had the constants modified to represent the more modern values given by Cox and Eilers (private communication). We also include a contribution from electron conduction.

The hydrogen component of the opacity is

$$\kappa_1 = 6.48 \times 10^{-3}\,\frac{(1+X)X\rho}{T_7^{4.25}}\,, \tag{B1}$$

where X is the fraction of hydrogen by weight, ρ is the density in grams per cubic centimeter, and T_7 is the temperature in units of 10^7 ° K. The helium component is

$$\kappa_2 = 186\rho(1+X)Y\left\{\frac{1.05 \times 10^{-3}}{T_7^3(10T_7+1)} + \frac{2-Y}{[0.15+T_7(300T_7-7)]^4}\right\}, \tag{B2}$$

where Y is the fraction of helium by weight.

The contribution due to heavy elements with a total masswise concentration Z is

$$\begin{aligned}\kappa_3 = 4.38 \times 10^3 Z\Big[\!\!\Big[&\{0.455[\rho(1+X)]^{1/2}+1\}\\ &\times\left[\frac{5.38T_7^2}{\rho(1+X)}+1\right]\left[\frac{1.34\times 10^5 T_7^5}{\rho(1+X)}+1\right]\left[1.44T_7^2+\frac{1}{(10T_7)^{3/2}}\right]\Big]\!\!\Big]^{-1/2},\end{aligned} \tag{B3}$$

and the scattering by free electrons is

$$\kappa_4 = 0.195(1 + X)\,. \tag{B4}$$

Combining these we obtain the total radiative opacity:

$$\kappa_r = \frac{(\kappa_1+\kappa_2)(\kappa_3+\kappa_4)+\kappa_3\kappa_4}{\kappa_1+\kappa_2+\kappa_3+\kappa_4} + \kappa_1 + \kappa_2 + \kappa_3 + \kappa_4\,. \tag{B5}$$

---

[2] The published formulae suffer from a typographical error.

1965ApJ...141.1019B

The conductive opacity is given by

$$\kappa_c^{-1}=\frac{T_7}{301.8}\{1+[0.004364(1+X)\rho T_7^{-3/2}]^{5/3}\}. \tag{B6}$$

This expression is a slight modification of the one given by Haselgrove and Hoyle (1959) which they constructed to fit the tabular values of Mestel (1950). It has within it, therefore, all the shortcomings of that theory.

The total combined effective opacity is given by

$$\kappa^{-1}=\kappa_r^{-1}+\kappa_c^{-1}. \tag{B7}$$

A comparison of our opacities with those computed by Cox and Eilers indicates agreement to within about 20 per cent for temperatures over 10^5 ° K, but closer agreement on the average.

APPENDIX C

CHEMICAL COMPOSITION VARIATIONS DURING HYDROGEN BURNING

The description of our computing technique (HFG) omits discussion of the details concerning the numerical treatment of nuclear reactions and their effects on chemical composition. Since certain aspects of the reactions, particularly the cross-sections, are subject to modification, it was felt best to dissociate them from the basic discussion, which may be presumed to have a more extended life. This report basically concerns hydrogen burning and therefore requires a review of this omission. It should be recalled that in the over-all computation the reaction rates are calculated once for each iteration of the physical variables, r_j, F_j, T_j, and q_j. This is graphically shown in the basic flow diagram (Fig. 2 of HFG). Thus the composition so derived is compatible only with the temperature and density given by the preceding iteration, and becomes definitive only after the final iteration. The flow diagram needs amendment in that, when the values of the physical variables have converged, these final values are used to recompute the reaction rates and composition.

The p-p chain of reactions is as follows:

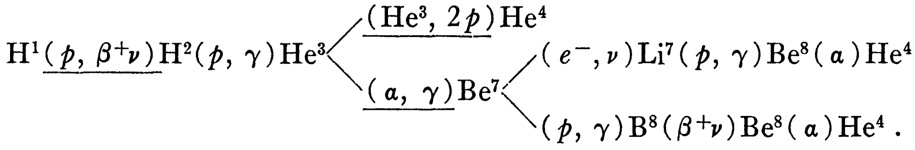

$$H^1\underline{(p,\beta^+\nu)}H^2(p,\gamma)He^3\begin{cases}\underline{(He^3,2p)}He^4\\ \underline{(\alpha,\gamma)}Be^7\begin{cases}(e^-,\nu)Li^7(p,\gamma)Be^8(\alpha)He^4\\ (p,\gamma)B^8(\beta^+\nu)Be^8(\alpha)He^4 .\end{cases}\end{cases}$$

In our calculations we treat the underlined reactions in detail but regard all others as proceeding instantaneously. In addition, the branching at Be^7 is treated numerically without, however, permitting either channel a finite duration.

In the CNO bi-cycle

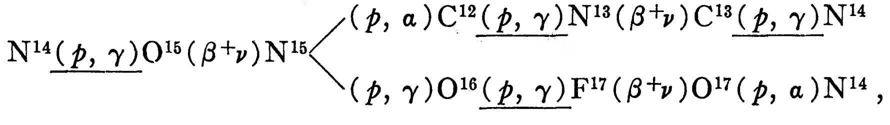

$$N^{14}\underline{(p,\gamma)}O^{15}(\beta^+\nu)N^{15}\begin{cases}(p,\alpha)C^{12}\underline{(p,\gamma)}N^{13}(\beta^+\nu)C^{13}\underline{(p,\gamma)}N^{14}\\ (p,\gamma)O^{16}\underline{(p,\gamma)}F^{17}(\beta^+\nu)O^{17}(p,\alpha)N^{14},\end{cases}$$

the underlined reactions are treated explicitly, together with the branching ratio at N^{15}. The (p,α) and (p,γ) reactions on N^{15} are otherwise treated as instantaneous.

We adopt the notation x_a for the abundance of any nuclear species a in grams per gram of mixture. The numerical subscript is the mass number of any of the species H^1, He^3, He^4, C^{12}, C^{13}, N^{14}, and O^{16}. The number of reactions between two species a and b, in moles per gram-second, is $R_{a,b}x_a x_b$ when $a\neq b$. When $a=b$, $R_{a,a}x_a^2$ gives twice this rate of reaction. The calculations of the composition as a function of time then requires the reaction rates $R_{1,1}$, $R_{3,3}$, $R_{3,4}$,

1965ApJ...141.1019B

$R_{1,12}$, $R_{1,13}$, $R_{1,14}$, and $R_{1,16}$, as well as the fraction f of N^{15} reactions that proceed to O^{16}. The branching at Be^7 is of concern only for the energy production because the neutrino losses differ on the two channels.

Adopting the assumptions and notation just described we may readily derive the following differential equation for the time variations of the concentrations:

$$\frac{dx_1}{dt} = -\tfrac{3}{2}R_{1,1}x_1{}^2 + R_{3,3}x_3{}^2 - R_{3,4}x_3x_4 - R_{1,12}x_1x_{12} - R_{1,13}x_1x_{13} - 2R_{1,14}x_1x_{14} - 2R_{1,16}x_1x_{16}\,, \tag{C1}$$

$$\tfrac{1}{3}\,\frac{dx_3}{at} = \tfrac{1}{2}R_{1,1}x_1{}^2 - R_{3,3}x_3{}^2 - R_{3,4}x_3x_4\,, \tag{C2}$$

$$\tfrac{1}{4}\,\frac{dx_4}{at} = \tfrac{1}{2}R_{3,3}x_3{}^2 + R_{3,4}x_3x_4 + (1-f)R_{1,14}x_1x_{14} + R_{1,16}x_1x_{16}\,, \tag{C3}$$

$$\tfrac{1}{12}\,\frac{dx_{12}}{dt} = -R_{1,12}x_1x_{12} + (1-f)R_{1,14}x_1x_{14}\,, \tag{C4}$$

$$\tfrac{1}{13}\,\frac{dx_{13}}{at} = R_{1,12}x_1x_{12} - R_{1,13}x_1x_{13}\,, \tag{C5}$$

$$\tfrac{1}{14}\,\frac{dx_{14}}{dt} = R_{1,13}x_1x_{13} - R_{1,14}x_1x_{14} + R_{1,16}x_1x_{16}\,, \tag{C6}$$

$$\tfrac{1}{16}\,\frac{dx_{16}}{dt} = fR_{1,14}x_1x_{14} - R_{1,16}x_1x_{16}\,. \tag{C7}$$

In converting these equations into difference equations for computational purposes we must use a method which assures general correctness even when the time step Δt greatly exceeds the mean life of one or more species. The simplest, though not necessarily the best, is the implicit scheme we adopt. If $\boldsymbol{x}$ is the vector whose components are the x_a, the differential equations (C1)–(C7) have the symbolic form

$$\frac{d\boldsymbol{x}}{dt} = \boldsymbol{F}(\boldsymbol{x}, t)\,. \tag{C8}$$

The difference equation corresponding to this is chosen in the form:

$$\boldsymbol{x} - \boldsymbol{x}^n = \Delta t\boldsymbol{F}(\boldsymbol{x}, t)\,, \tag{C9}$$

where the superscript $\boldsymbol{n}$ is placed on a quantity evaluated at the earlier epoch, n, and where the absence of a superscript on $\boldsymbol{x}$ and t means that they are evaluated at the advanced epoch, $n+1$. We assume that $\boldsymbol{x}^n$, t, and Δt are known. The unknown, $\boldsymbol{x}$, occurs also in the right-hand member of equation (C9), so that a scheme of iteration is required. The function $\boldsymbol{F}$ involves all the reaction rates $R_{a,b}$, which are computed from the currently best available values of T and ρ at the advanced time t.

The desirability of using the implicit scheme given by equation (C9) depends on considerations which, while reasonably well known, bear some repetition here. Simply for purposes of explanation and illustration consider the differential equation

$$\frac{dx}{dt} = a(t) - xb(t)\,. \tag{C10}$$

1965ApJ...141.1019B

It bears a generic resemblance to the system with which we are concerned. For example, the equilibrium (approximate) solution

$$x = a(t)/b(t) \tag{C11}$$

will represent the true solution with high precision if the ratio varies sufficiently slowly. This feature is certainly common to all of the variables x_3, x_{12}, x_{13}, x_{14}, and x_{16}. Consider now the explicit scheme

$$x - x^n = \Delta t(a - bx^n)\,, \tag{C12}$$

where, as before, x refers to epoch $n + 1$. Then

$$x = x^n(1 - b\Delta t) + a\Delta t\,, \tag{C13}$$

where for convenience we treat a and b as constants. An alternative way of writing the solution is

$$x - \frac{a}{b} = \left(x^n - \frac{a}{b}\right)(1 - b\Delta t)\,. \tag{C14}$$

The parameter b is the reciprocal "mean life" of x. If Δt greatly exceeds $1/b$, the error of the equilibrium solution (C11) changes sign, and, what is disastrous, grows enormously in absolute size. Since in our evolutionary calculations Δt very often exceeds some mean lives by large factors, scheme (C12) is unacceptable. On the other hand, if we adopt the implicit scheme

$$x - x^n = \Delta t(a - bx)\,, \tag{C15}$$

the solution analogous to expression (C14) becomes

$$x - \frac{a}{b} = \left(x^n - \frac{a}{b}\right)\Big/(1 + b\Delta t)\,. \tag{C16}$$

Now the error of the equilibrium solution decreases substantially. For small Δt there is no preference, but for large Δt equation (C15) is decisively superior to equation (C12), in spite of the necessity of iterating which its use introduces in the general problem.

The solution of the difference equations corresponding to equation (C9) may be carried out by various techniques. One that we have found convenient and reasonably rapid for machine programming computes the values of the concentrations in three steps within a larger iterative cycle. Suppose that x_1 and x_4 are given (by estimates initially or by a previous iteration). The differential equations (C4)–(C7) correspond to the following difference equations of the form (C9):

$$x_{12} - x_{12}{}^n = 12\Delta t[-R_{1,12}x_1x_{12} + (1 - f)R_{1,14}x_1x_{14}]\,, \tag{C17}$$

$$x_{13} - x_{13}{}^n = 13\Delta t[R_{1,12}x_1x_{12} - R_{1,13}x_1x_{13}]\,, \tag{C18}$$

$$x_{14} - x_{14}{}^n = 14\Delta t[R_{1,13}x_1x_{13} - R_{1,14}x_1x_{14} + R_{1,16}x_1x_{16}]\,, \tag{C19}$$

$$x_{16} - x_{16}{}^n = 16\Delta t[fR_{1,14}x_1x_{14} - R_{1,16}x_1x_{16}]\,. \tag{C20}$$

These equations are linear in the unknowns x_{12}, x_{13}, x_{14}, and x_{16}, and can be solved for these at once. Corresponding to equation (C2) we similarly derive a difference equation

$$x_3 - x_3{}^n = 3\Delta t[\tfrac{1}{2}R_{1,1}x_1{}^2 - R_{3,3}x_3{}^2 - R_{3,4}x_3x_4]\,, \tag{C21}$$

1965ApJ...141.1019B

which is quadratic in, and may be solved for, the unknown x_3. Finally, subtracting equation (C1) from equation (C1) and writing in difference form we get

$$x_1 - x_1^n - \tfrac{1}{3}(x_3 - x_3^n) = \Delta t[-2R_{1,1}x_1^2 + 2\,R_{3,3}x_3^2 - x_1 \times (R_{1,12}x_{12} + R_{1,13}x_{13} + 2\,R_{1,14}x_{14} + 2\,R_{1,16}x_{16})] \,. \qquad \text{(C22)}$$

This quadratic equation gives an improved value of x_1, which may be used to compute an improved x_4 from the condition of conservation:

$$\sum_a x_a = 1 \,. \qquad \text{(C23)}$$

The resulting values of x_1 and x_4 may now be tested for precision by comparing them with the input values. If they differ from the latter by more than a prescribed tolerance the whole procedure must be repeated.

The numerical values of constants used in calculating reaction rates have been taken from various sources. For the *p-p* reaction we use

$$R_{1,1} = 7.07 \times 10^{-9}\,\rho f_{pp} T_7^{-2/3} \times (1 + 0.026T_7^{1/3} + 0.037T_7^{2/3} + 0.0065T_7)\exp(-15.69/T_7^{1/3}) \,, \qquad \text{(C24)}$$

where

$$f_{pp} = 1 + 0.00762(\rho/T_7^3)^{1/2} \qquad \text{(C25)}$$

is the electron-screening factor. Equation (C24) is essentially that given by Burbidge, Burbidge, Fowler, and Hoyle (1957), where the constant factor is obtained by increasing the value of S_0 given by them by a factor $\frac{336}{285}$, as suggested by Fowler (1960). The electron-screening factor (C25) is taken from Fowler (1960). The rate of energy generation is $\frac{3}{2}\,\epsilon_{1,1}R_{1,1}x_1^2$ since each *p-p* reaction leads to the consumption of three protons. The energy release is 2.23 MeV per proton consumed, or

$$\epsilon_{1,1} = 2.15 \times 10^{18}\ \text{erg/(mole of H}^1\text{ consumed)} \,. \qquad \text{(C26)}$$

The reaction rates $R_{3,3}$, $R_{3,4}$, $R_{1,12}$, $R_{1,13}$, $R_{1,14}$, and $R_{1,16}$ are all computed from

$$R_{a,b} = \frac{4.3425 \times 10^5 f_0 S_0}{A\,A_a A_b Z_a Z_b}\,\rho\,\tau^2 e^{-\tau}\left(1 + \frac{5}{12\tau} - \frac{35}{288\tau^2}\right), \qquad \text{(C27)}$$

where

$$A = \frac{A_a A_b}{A_a + A_b},$$

$$\tau = 19.71\left(\frac{A Z_a^2 Z_b^2}{T_7}\right)^{1/3}, \qquad \text{(C28)}$$

and f_0 is the electron-screening factor. The values of the product $f_0 S_0$ have been taken from Table II of Fowler (1960).

The rates of the two reactions on Be^7 are calculated for a determination of the branching ratio, the (p, γ) reaction rate $R_{1,7}$ being of the form (C27) and the (e^-, ν) reaction rate being calculated from

$$R_{07} = 8.6 \times 10^{-11}\rho T_7^{-1/2}\ \text{molar reactions/sec} \,.$$

This is essentially equation (6.3.19) of Cameron (1957), with the constant converted from Cameron's units to ours. The value of $f_0 S_0$ for $R_{1,7}$ is from Fowler.

Many of these reaction rates are to be replaced by newer improved values and are referred to here only for the sake of defining the values used in the principal part of this report.

APPENDIX D

CHEMICAL HOMOGENIZATION OF CONVECTIVE REGIONS

The theory of convection suggests that an adequate allowance for the effect of mixing may be obtained by a complete homogenization of the convective region for each constituent. It is presumed that the convective mixing time scale is short compared to the time scale characterizing the processes, such as nuclear reactions and motion of the interfaces bounding convective regions, that tend to produce compositional changes.

Let the convective region be bounded by two mass points within the star, m_1 and m_2, which we may assume to be varying in time subject to the condition $m_2 > m_1$. Then the mass of the convective region is

$$\Delta m = m_2 - m_1 . \tag{D1}$$

Let the value of the masswise concentration of a particular constituent be x in the convective region, x_1 immediately on the radiative side of the inner boundary, and x_2 immediately on the radiative side of the outer boundary. Finally let $(\partial x/\partial t)_{\text{th}}$ be the point-to-point rate at which thermonuclear reactions tend to change the concentration x.

The quantities x_1 and x_2 may individually or both be equal to x provided they describe matter left behind in a radiative region by a boundary receding into a convective region. Thus

$$x_1 = x \text{ if } \frac{dm_1}{dt} > 0 \qquad \text{and} \qquad x_2 = x \text{ if } \frac{dm_2}{dt} < 0 .$$

Then homogenization requires that

$$\frac{d}{dt}(x\Delta m) = x_2 \frac{dm_2}{dt} - x_1 \frac{dm_1}{dt} + \int_{m_1}^{m_2} \left(\frac{\partial x}{\partial t}\right)_{\text{th}} dm . \tag{D2}$$

The implementation in an actual numerical calculation involves, at best, various inconvenient complications. We now describe the approximation used in our technique.

a) *Convective envelope.*—In this case $m_2 = M$, the mass of the whole star. In most applications, but possibly not in all those to be encountered in the future, the effect of nuclear reactions is negligible. Also the changes in position of the boundary m_1 with time are not seriously affected by the homogenization through the stability condition since changes in composition are relatively small. Let x_e be the concentration of any constituent within the envelope. As long as the foregoing conditions are fulfilled, we will proceed by first doing the reactions as a local point-to-point operation giving us a set of local values $x_e'(\xi)$ throughout the envelope as an intermediate stage, and then deriving an average value of x_e for the homogenized envelope from

$$x_e = \frac{1}{\Delta m} \int_{m_1}^{M} x_e' dm . \tag{D3}$$

It is possible that advanced evolutionary phases will lead to vitiation of the assumptions made and that as a result a more refined scheme will be needed.

b) *Convective core.*—In the core case $m_1 = 0$ and $m_2 = \Delta m = m_c$, where m_c is the mass of the core. If x_c is the concentration of any constituent in the core, equation (D2) may now be written in a modified form:

$$\frac{dx_c}{dt} = \frac{x_2 - x_c}{m_c} \frac{dm_c}{dt} + \frac{1}{m_c} \int_0^{m_c} \left(\frac{\partial x}{\partial t}\right)_{\text{th}} dm . \tag{D4}$$

Two cases arise. If the core is shrinking masswise $x_2 - x_c = 0$ and

$$\frac{dx_c}{dt} = \left\langle \left(\frac{\partial x}{\partial t}\right)_{\text{th}} \right\rangle , \tag{D5}$$

1965ApJ...141.1019B

where the right-hand member is the rate of change due to thermonuclear reactions, calculated at epoch $n+1$, averaged over the mass of the core. Then the normal technique described in Appendix C is applicable using mass averages of the reaction rates $R_{a,b}$. When the core is growing, a sweep-up effect arises which is described by the first term on the right in equation (D4). The procedure in this case is more complex but can be formally reduced to the standard process of Appendix C as follows. In order to obtain the desired result, we find it more convenient to proceed along a new line of argument. Let m_0 be a fixed mass point which at a given instant of time is at least as large as m_c, the mass inclosed in the core at that instant. We now consider the integrated value of x from the center to m_0, which includes the homogeneous contribution from the core plus a contribution from the shell lying between m_c and m_0. Under these conditions at the given instant the following relation is valid:

$$\frac{d}{dt}\int_0^{m_0} x\,dm = \int_0^{m_0}\left(\frac{\partial x}{\partial t}\right)_{\text{th}} dm = m_0\left\langle\left(\frac{\partial x}{\partial t}\right)_{\text{th}}\right\rangle . \tag{D6}$$

In this equation the average $\langle(\partial x/\partial t)_{\text{th}}\rangle$ includes a contribution from the core itself and a contribution from the shell between m_c and m_0. We now apply this result to the whole time interval between t^n and t^{n+1}, and we identify m_0 with m_c^{n+1}. The integral of the left-hand side of equation (D6) over this time interval then becomes

$$x_c^{n+1} m_c^{n+1} - \left(x_c^n m_c^n + \int_{m_c^n}^{m_c^{n+1}} x^n\,dm\right).$$

In accordance with our standard procedure outlined in Appendix C, we use the values of the reaction rates at epoch $n+1$ to represent their values during the whole time interval. Therefore we obtain

$$x_c^{n+1} m_c^{n+1} - \left(x_c^n m_c^n + \int_{m_c^n}^{m_c^{n+1}} x^n\,dm\right) = m_c^{n+1}\Delta t\left\langle\left(\frac{\partial x}{\partial t}\right)_{\text{th}}\right\rangle .$$

This expression reduces to

$$x_c^{n+1} = x_c^n + \frac{1}{m_c^{n+1}}\int_{m_c^n}^{m_c^{n+1}} (x^n - x_c^n)\,dm + \left\langle\left(\frac{\partial x}{\partial t}\right)_{\text{th}}\right\rangle \Delta t . \tag{D7}$$

It must be emphasized that x_c^n is a constant in the integration, but x^n is the variable concentration as a function of m, the independent variable of integration. The regular formalism may then be used if we replace x_c^n by x_c^*, where

$$x_c^* = x_c^n + \frac{1}{m_c^{n+1}}\int_{m_c^n}^{m_c^{n+1}} (x^n - x_c^n)\,dm . \tag{D8}$$

The advantage of this substitution over the more accurate time-centered scheme is that the sweep-up effect is computed exclusively with known quantities, namely, those given for the earlier epoch t^n.

APPENDIX E

STARTING A NEW EVOLUTIONARY SEQUENCE

The mathematical problem devolving from the time-dependent evolution of a stellar configuration is both a boundary-value and an initial-value problem. Specification of boundary conditions is an integral part of the calculation of the evolutionary sequence (see HFG). The formulation of initial values is a separate problem which, in turn, has different aspects that we now consider.

Expressed mathematically, the different variables describing the structure must be specified as functions of some independent variable in a manner which is both compatible with the

1965ApJ...141.1019B

boundary conditions and subject to those equations that do not involve the time. The latter goal may, as we shall show, be achieved by specifying some of the variables and using the time-independent equations to compute the rest. The manner in which this is done is, in a practical way, greatly dependent on the nature of the problem under investigation. If a program of study of pre-main-sequence evolution is contemplated, the starting procedure becomes a highly complex and completely decisive part of the whole task. On the other hand, if a program of thermonuclearly controlled evolution is under way, the starting assignment is considerably different. The latter approach is the subject of this Appendix, while the former is under investigation by one of us (P. B.).

We choose a Lagrangian coordinate ξ as the independent variable with an assigned relation between it and the mass, $m(\xi)$, such that $0 \leq \xi \leq 1$. It will now be shown that, if the run of the density is initially specified as a function of ξ, all the other physical variables throughout the star can be derived from the time-independent equations of stellar structure.

The radius, r, is derived by integrating the equation

$$\frac{1}{4\pi\rho}\frac{dm}{d\xi} = r^2 \frac{\partial r}{\partial \xi}. \tag{E1}$$

The pressure as a function of ξ then follows from integrating the equation of hydrostatic equilibrium:

$$P = \int_{\xi}^{1} \frac{Gm\rho}{r^2}\frac{\partial r}{\partial \xi}\, d\xi. \tag{E2}$$

Using the equation of state we may then determine T as a function of ξ, provided a complete specification of the chemical composition has been made. The luminosity $l(\xi)$ can then be computed from the temperature gradient, provided that the radiative gradient is stable. Should the resulting gradient be unstable the assumed relation between ρ and ξ is inadmissible. In convective regions the value of l at this point of the calculation is arbitrary, in principle, but can be adjusted to achieve reasonable continuity and thus provide a satisfactory first approximation.

In practice, however, the program just outlined can be applied in a modified manner when an evolutionary calculation is to be started at a point near the main sequence. In such a case we may apply a homology transformation in r, q, and p (for definitions of these quantities see HFG) from a previously existing source configuration, part of a sequence for another mass and composition. Such a transformation insures that equations (E1) and (E2) are satisfied. The method, however, has limitations in that only a relatively small change in mass and composition in passing from the source configuration to the new configuration is permitted, since otherwise the new configuration falls outside the region of convergence of the iterative procedure described in HFG.

We specify a total mass M, initial radius R, and homogeneous chemical composition represented by the concentrations x_a of certain nuclear species. To calculate the mass $m(\xi)$, we use an analytic expression for $m'(\xi)$ (where $m'(\xi) = dm/d\xi$) which is so chosen that ξ is approximately proportional to r. The precise expression for $m'(\xi)$ is unimportant, so long as $m(\xi) \propto \xi^3$ as $\xi \rightarrow 0$ and $m(1) = M$. Numerical integration of $m'(\xi)$ gives $m(\xi)$ for some set of equally spaced values of ξ, and a table of differences to the sixth order permits us to calculate $m(\xi)$ for intermediate ξ-values. This is needed for any temporary mesh point that is inserted, and also for the mesh points representing boundaries of the convective regions, since the locations of these change from epoch to epoch. Let $\mathfrak{C}_0$ denote the source configuration and $\mathfrak{C}$ the new initial configuration to be derived. Let the subscript zero denote values from the source configuration. Then a homology transformation from $\mathfrak{C}_0$ to $\mathfrak{C}$ gives

$$r(\xi) = r_0(\xi)\frac{R}{R_0}, \tag{E3}$$

$$q(\xi) = q_0(\xi)\left(\frac{M}{M_0}\right)^{1/3}\left(\frac{R_0}{R}\right), \tag{E4}$$

$$p(\xi) = p_0(\xi)\left(\frac{M}{M_0}\right)^{1/2}\left(\frac{R_0}{R}\right). \tag{E5}$$

Values of the temperature, $T(\xi)$, and internal energy per gram, $E(\xi)$, are obtained from the equation of state. The luminosity, $l(\xi)$, could then be derived from the temperature gradient; however in practice a scaling of the luminosity of $\mathfrak{C}_0$ according to a crude mass-luminosity relation suffices to give a first approximation to the luminosity for $\mathfrak{C}$.

Because of complexities inherent in stellar structure (e.g., incomplete ionization, the behavior of the opacity, presence of convective regions), we find it desirable to use a $\mathfrak{C}_0$ as close to $\mathfrak{C}$ as possible. If they differ so much that a successful transformation $\mathfrak{C}_0 \rightarrow \mathfrak{C}$ cannot be made directly, we transform through several stages ($\mathfrak{C}_0 \rightarrow \mathfrak{C}_1 \rightarrow \mathfrak{C}_2 \rightarrow \ldots \rightarrow \mathfrak{C}$). Allowing each intermediate stage to run for a few epochs permits transient numerical disturbances to damp out partially.

Before $\mathfrak{C}$ can be used to begin the evolutionary calculation, the model must be provided with four standard model atmospheres, all computed for the composition specified for the interior. Each atmosphere calculation depends on assumed values of the radius R and the surface luminosity L, which are near, but in general not equal to, the R and L of the stellar model. We choose two values of the radius, R' and R'', and two values of the luminosity, L' and L'', such that

$$R'' = 1.15R', \qquad L'' = 1.15L', \qquad R' \leqq R \leqq R'', \qquad L' \leqq L \leqq L''.$$

Then the four model atmospheres are calculated for (R', L'), (R', L''), (R'', L'), and (R'', L''). The true values of R and L for the model star are intermediate. The external boundary conditions for the interior integration are given by an "effective" atmosphere which is interpolated among the four standard atmospheres. At this point $\mathfrak{C}$ is not a true stellar model in that it does not satisfy the full set of equations of stellar structure; however, all the necessary variables have been provided so that it can serve as a starting point for the solution of the time-dependent equations.

REFERENCES

Aller, L. H. 1961, *Abundances of the Elements* (New York: Interscience Publishers), p. 179.
Bos, W. H. van den. 1960, *J. d. Obs.*, **43**, 145.
Burbidge, E. M., Burbidge, G. R , Fowler, W. A., and Hoyle, F. 1957, *Rev. Mod. Phys.*, **29**, 563.
Cameron, A. G. W. 1957, *Stellar Evolution, Nuclear Astrophysics, and Nucleogenesis* (2d. ed.; Atomic Energy of Canada Ltd., CRL-41, Chalk River), p. 174.
Chandrasekhar, S. 1939, *An Introduction to the Study of Stellar Structure* (Chicago: University of Chicago Press), chap. xi.
Eggen, O. J. 1960, *M.N.*, **120**, 563.
Elste, G., and Jugaku, J. 1957, *Ap. J.*, **125**, 742.
Fowler, W. A. 1960, *9th Liège Symposium*, pp. 207–218.
Harris, D L. 1963, *Basic Astronomical Data*, ed. K. Aa. Strand (Chicago: University of Chicago Press), p. 269
Harris, D. L., Strand, K. Aa., and Worley, C. E. 1963, *Basic Astronomical Data*, ed. K. Aa. Strand (Chicago: University of Chicago Press), p. 276.
Haselgrove, C. B., and Hoyle, F. 1959, *M.N.*, **119**, 112.
Henyey, L. G , Forbes, J. E., and Gould, N. L. 1964, *Ap. J.*, **139**, 306.
Henyey, L. G., LeLevier, R., and Levée, R. D. 1955, *Pub. A.S.P.*, **67**, 154.
———. 1959, *Ap. J.*, **129**, 2.
Hoerner, S. von. 1957, *Zs. f. Ap* , **42**, 273.
Johnson, H. L., and Morgan, W. W 1953, *Ap. J.*, **117**, 313
Kamp, P. van de. 1958, *Hdb. d. Phys.*, Vol. **50**, ed. S. Flügge (Berlin: Springer-Verlag), p 221.
Keller, G , and Meyerott, R. E. 1955, *Ap. J.*, **122**, 32.
McDougall, J., and Stoner, E. C. 1938, *Phil. Trans. Roy. Soc.*, **A237**, 67.
Mestel, L. 1950, *Proc Cambridge Phil. Soc* , **46**, 331.
Popper, D. M 1959, *Ap. J.*, **129**, 647.